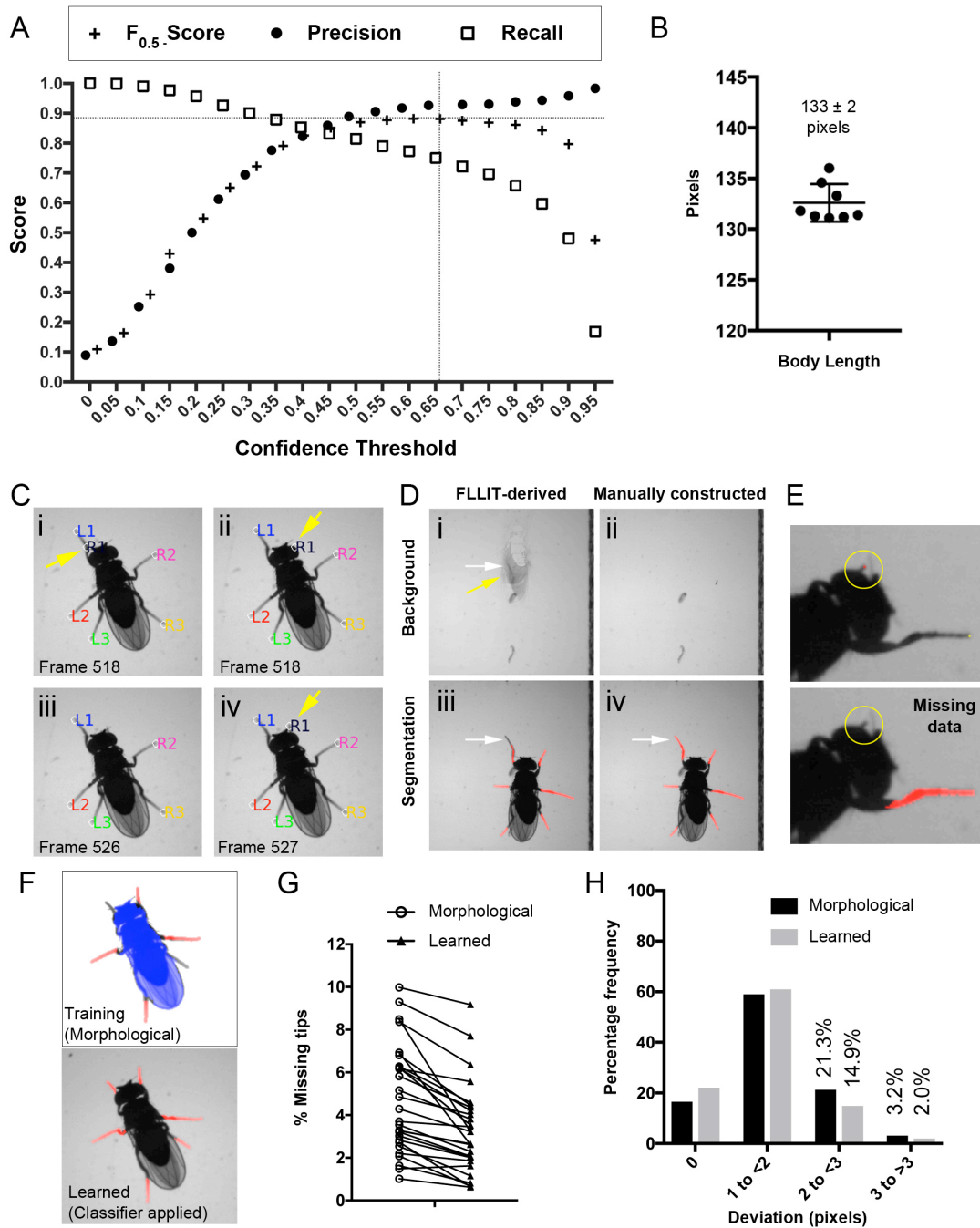


**Figure S1. System setup.** **A.** Experimental setup used for video capture. Videos taken with the side view camera (that is synchronised with the top/bottom view camera) were used for occasional reference, but not for tracking. **B.** Top view of the sample stage.

Related to Figure 1.



**Figure S2. Ground truth demonstrates the accuracy of segmentation and tracking results reported by FLLIT. A.** Average  $F_{0.5}$ , precision and recall scores for segmentation, at various confidence thresholds ( $n = 18$  images from 8 videos). Classifier performance peaked at thresholds of 0.6-0.65. The more stringent threshold of 0.65 was selected for subsequent analyses. **B.** Body length measurements in pixels (anterior to wing posterior) taken under our default video recording parameters. Bars represent the means and standard deviations. **C.** Example of error correction for misidentification errors. i) In frame 518, leg claw R1 was misidentified to the left leg (yellow arrow) during retraction of leg R1; this error was perpetuated for multiple frames while the R1 leg was occluded. ii) A single correction was made in frame 518 (yellow arrow and circle labelled R1), >20 pixels away from the location of

the misidentification. iii) After the correction (from frames 519 to 526), R1 was subsequently reported as missing, because no segmented region was found within 20 pixels of the corrected R1 position in frame 518. iv) The correctly tracked position for R1 reappears in frame 527, <20 pixels away from the correction made in frame 518. **D.** Effect of suboptimal automated background generation on segmentation performance. (i) The FLLIT-generated background left traces of the fly silhouette, compared to (ii) a background that was manually constructed using image processing. (iii) Poor background subtraction and segmentation as a result of (i). (iv) Improved segmentation after subtracting a manually constructed background. **E.** Manual annotation of the front left leg (top image; red dot within the yellow circle) by a human user, compared to segmentation failure leading to marking the left front leg claw as “absent” by the algorithm, and thus resulting in missing data (bottom image; yellow circle). **F.** *Drosophila* silhouette segmented using solely morphological operations (Top; the red and blue pixels constitute a set of highly confident positive and negative training samples; see also Fig 1B), and the same silhouette segmented by application of a classifier after training (Bottom). **G.** Percentage of missing data for each video when using morphological operations alone vs after learning (n = 29 videos, 15,166 frames, 90,996 legs). **H.** Frequency distribution of the deviation (in pixels) between computationally and manually-derived leg claw positions when using morphological operations alone vs after application of a classifier (n= 106 frames, 636 leg tips from two videos). *Abbreviation: FLLIT, Feature Learning-based Limb segmentation and Tracking.*

Related to Figure 2.

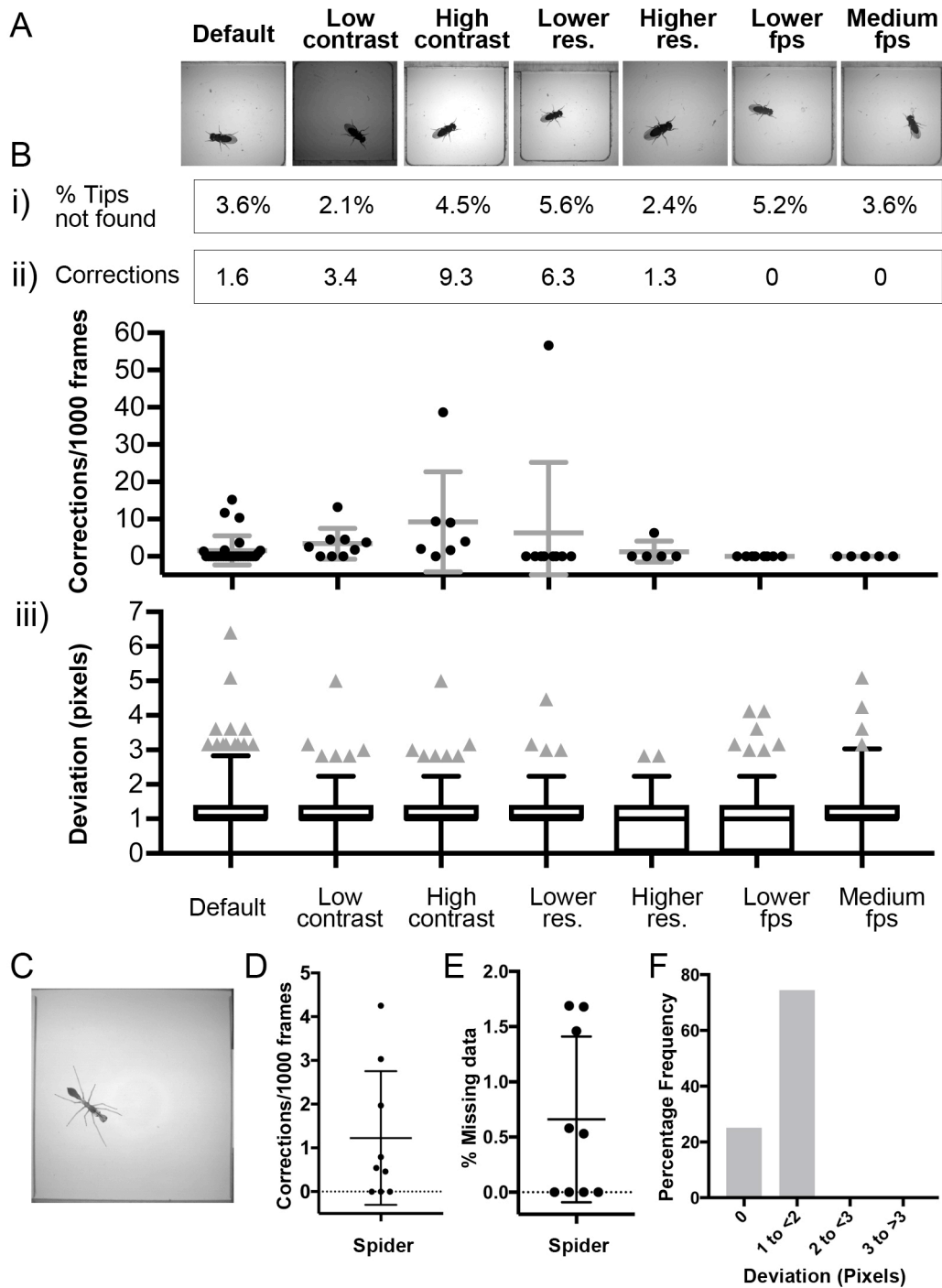


**Figure S3. Robustness testing of FLLIT by altering recording parameters and application of FLLIT to other arthropods.** **A.** Representative images from videos of wild-type *Drosophila* recorded under various recording settings that were manually annotated and analysed in (B). Default setting: default lighting/contrast, default resolution (10 mm square field of view), 1000 frames per sec (fps); low contrast (decreased light intensity) versus high contrast (increased light intensity); lower resolution (12 mm field of view) versus higher resolution (9 mm); low frame rate (250 fps) versus medium frame rate (500 frames per

second). **B.** (i) Number of leg tips not found, and (ii) Number of corrections required in videos of wild-type *Drosophila* monitored under different recording parameters. Default setting (n = 29 videos, 15,166 frames), low contrast (n = 9 videos, 5,678 frames), high contrast (n = 7 videos, 4,664 frames), lower resolution (n = 9 videos, 4,596 frames), higher resolution (9 mm) (n = 5 videos, 3,473 frames). 250 fps (n = 8 videos, 1,331 frames) and 500 fps (n = 5 videos, 1,389 frames). The graph depicts the number of corrections required per 1,000 frames, with error bars representing the means and standard deviations. (iii) Deviation (in pixels) between computationally and manually-derived leg-tip positions under the recording settings shown in (A). Data are represented as box and whiskers plots showing the 2.5 to 97.5 percentiles, with the >97.5 percentile points indicated using triangles. Settings: Default (n = 636 legs), low contrast (n = 390 legs), high contrast (n = 456 legs), lower resolution (n = 324 legs), higher resolution (n = 306 legs), 250 fps (n = 360 legs) and 500 fps (n = 186 legs). Bars represent the means and standard deviations. **C.** Representative images of the pixel resolution of *Myhmaplata plataleoides* salticid spider leg tips, at the recording settings used in this study. Red and green insets are 10 pixels wide and show the respective boxed regions in the yellow-boxed image. **D.** Number of corrections required for misidentified legs, normalised to per 1,000 frames (mean = 1.2 corrections/1000 frames; n = 9 videos, 12,683 frames, 101,464 legs). **E.** % missing data in each video after error correction. **F.** Frequency distribution of the deviation (in pixels) between computationally and manually-derived leg tip positions (n = 167 frames, 1,336 leg tips from 3 videos). Bars represent the means and standard deviations.

See also Video S1.

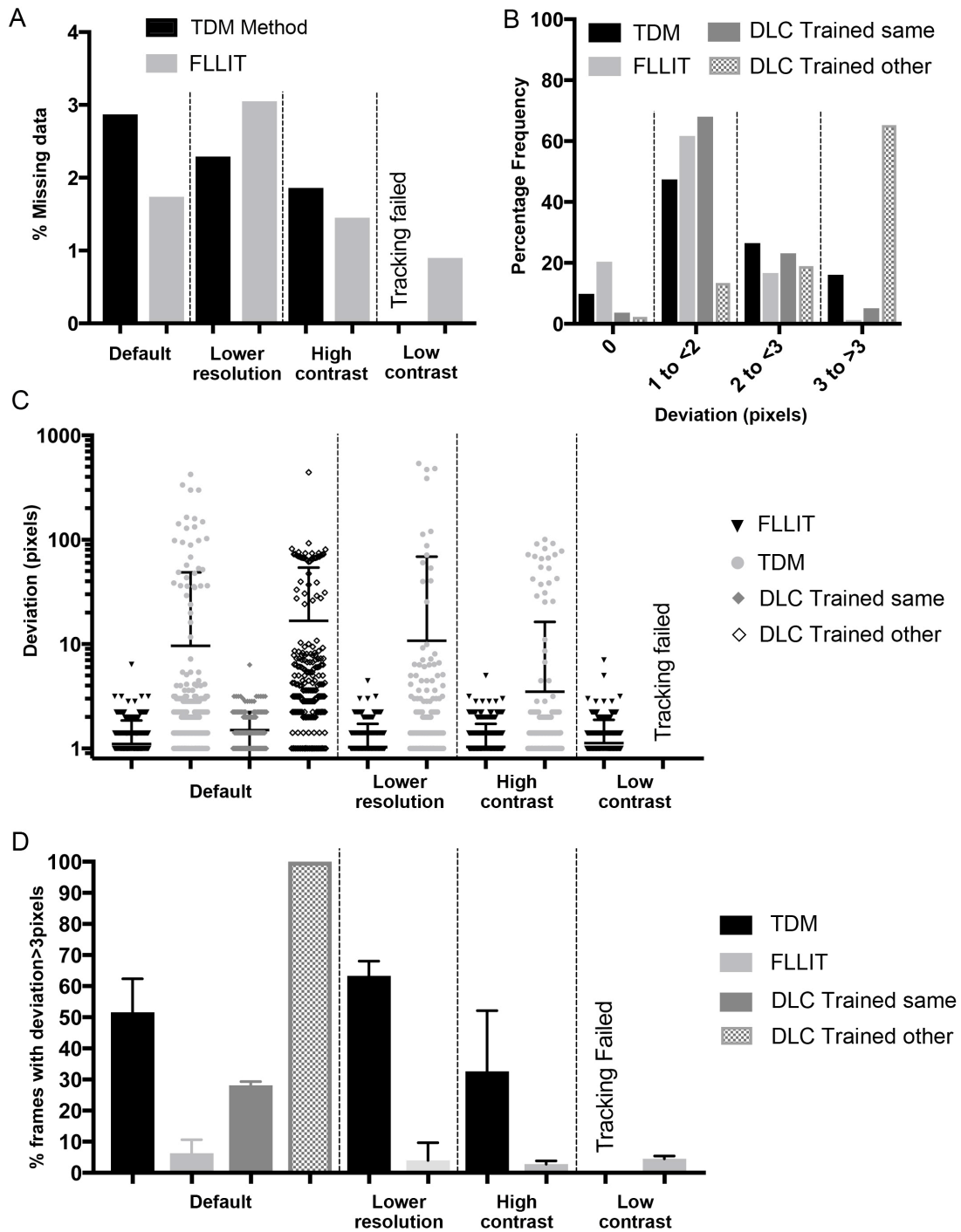


**Figure S4. Side-by-side comparison of method performance.** **A.** Percentage missing data for ground truth videos taken under different recording parameters, when tracked with either the method from Isakov *et al*<sup>6</sup> (thresholding and dynamic masking (TDM)) or using FLLIT. Settings: Default (n = 2 videos, 730 frames), lower resolution (n = 2 videos, 938 frames), high contrast (n = 2 videos, 1,562 frames), low contrast (n = 2 videos, 1,322 frames). Only frames from videos where the fly walked sufficiently close to the centre of the frame could be tracked with TDM. Tracking failed for all low contrast videos. **B.** Frequency distribution of the deviation (in pixels) between computationally tracked and manually annotated leg-tip

positions, using either TDM, FLLIT or DeepLabCut (DLC, trained either on the same video or on a different video recorded under the same settings) (n = 420 legs, 2 videos; Default settings). **C.** Deviation (in pixels) between computationally tracked and manually annotated leg-tip positions, using either TDM, FLLIT or DeepLabCut (DLC, trained either on the same video or on a different video recorded under the same settings). Default setting (n = 2 videos, 420 legs), lower resolution (n = 2 videos, 276 legs), high contrast (n = 2 videos, 456 legs), low contrast (n = 2 videos, 390 legs). **D.** Percentage of frames containing at least one leg that deviated >3 pixels from the manually annotated position, when tracked using either TDM, FLLIT or DeepLabCut (DLC, trained either on the same video or on a different video recorded under the same settings). Default setting (n = 2 videos, 420 legs), lower resolution (n = 2 videos, 276 legs), high contrast (n = 2 videos, 456 legs), low contrast (n = 2 videos, 390 legs). Bars represent the means and standard deviations.

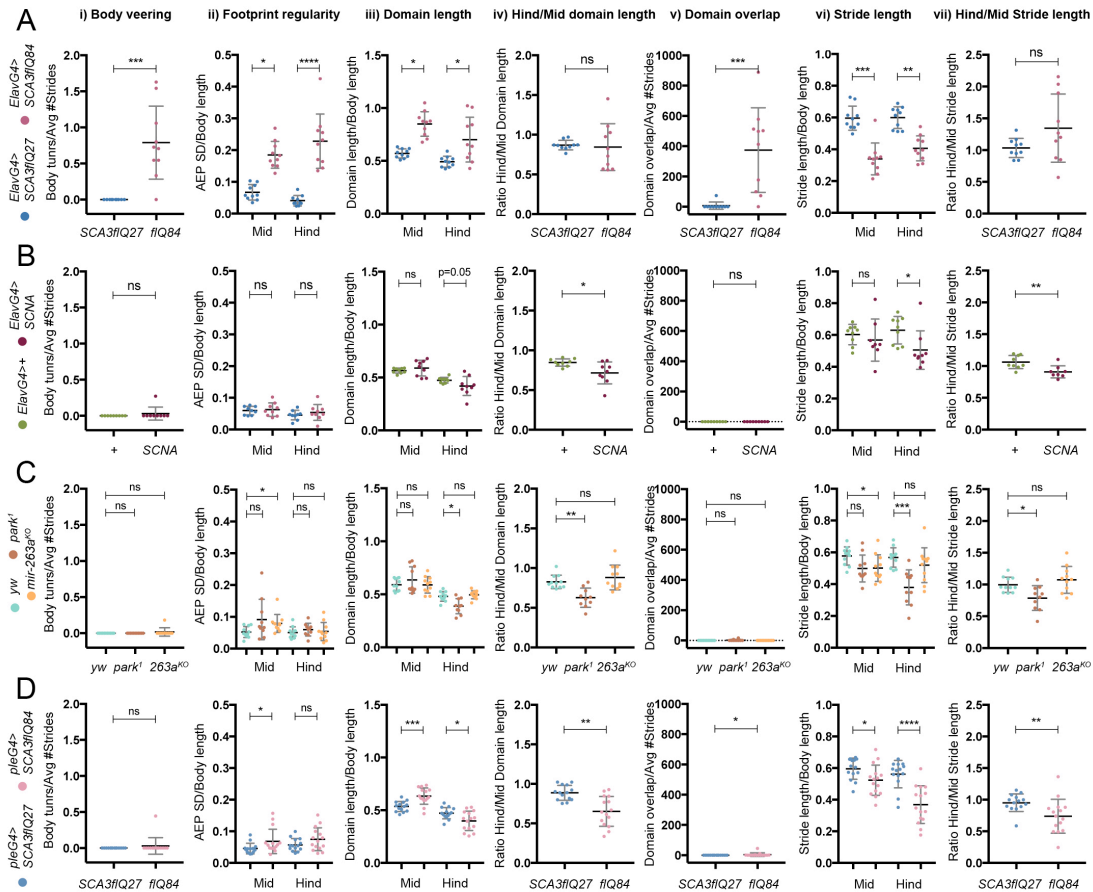


**Figure S5. Characterisation of gait in fly models of Spinocerebellar ataxia 3 and Parkinson's Disease.** (A-D) Dot plots of the respective gait parameters shown in Figure 3. The genotypes as indicated (coloured as in Fig. 3A) were analysed for the following gait parameters: (i) Body veering (Number of body turns normalised to the average number of strides per leg), (ii) Footprint regularity (Standard deviations of the anterior extreme position, normalised to body length), (iii) Leg domain length normalised to body length, (iv) Average ratio of the hind vs mid domain length of the right and left sides, (v) Number of pixels overlapping between leg domains, normalised to the average number of strides per leg), (vi) Stride lengths of the mid and hind legs normalised to body length, (vii) Average ratio of the hind vs mid stride lengths of the right and left sides. \* $P < 0.05$ , \*\* $P < 0.01$ , \*\*\* $P < 0.001$ , \*\*\*\* $P < 0.0001$ . Genotypes examined: *Elav-Gal4>SCA3-flQ27* ( $n = 10$ ), *Elav-Gal4>SCA3-flQ84* ( $n = 10$ ), *Elav-Gal4>+* ( $n = 9$ ), *Elav-Gal4>SCNA* ( $n = 9$ ), *yw* ( $n = 11$ ), *park<sup>1</sup>* ( $n = 10$ ), *mir-263a<sup>KO</sup>* ( $n = 11$ ), *ple-Gal4>SCA3-flQ27* ( $n = 14$ ), *ple-Gal4>SCA3-flQ84* ( $n = 15$ ). For panels with 2 genotypes (A, B, D), data were analysed using a non-parametric Mann-Whitney test. For panels with 3 genotypes (C), data were analysed using a non-parametric Kruskal-Wallis test with Dunn's multiple comparisons *post-hoc* test. Bars represent the means and standard deviations.

Related to Figure 3.



